Convection during Thermally Unstable Solidification of Pb-Sn in a Magnetic Field

H. SONG, S.N. TEWARI, and H.C. de GROH III

Convection and macrosegregation in directionally solidified hypoeutectic Pb-38 wt pct Sn and hypereutectic Pb-64.5 wt pct Sn have been examined during upward and downward growth. Temperature fluctuations are observed along the length of the melt column during downward growth. With increasing Rayleigh number, these fluctuations change from none, to cyclic, to time periodic having multiple harmonics, and finally to random. At the higher convective driving force of 350 K temperature inversion, the transverse magnetic field decreased convective levels, strong random temperature fluctuations (flows) becoming smaller and periodic. The maximum field of 0.45 T was unable to completely eliminate convection. For the lower convective driving force of 150 K temperature inversion, the 0.05 T magnetic field decreased flows, and at 0.15 T, the field caused a dramatic decrease in the characteristic frequency of the temperature fluctuations, indicating a change in the nature of the flow, the waveform of the temperature fluctuations changing from sinusoidal to a pulsed wave. Temperature fluctuations and time delays between thermocouples were used to estimate flow velocities. Irrespective of the convection in the bulk melt (ahead of the mushy zone), longitudinal macrosegregation occurs only if the interdendritic melt mixes with the bulk melt.

I. INTRODUCTION

MACROSEGREGATION during dendritic growth of alloys is caused by convection in the bulk and interdendritic melt, settling or floating of dendrite fragments, and the fluid flow due to solidification shrinkage. Directional solidification experiments have been used to study relationships between thermosolutal convection and macrosegregation in a range of binary metallic alloys.[1–11] Direct visual observation of convection during dendritic growth has been limited to transparent model analogues, such as NH_4Cl+H_2O.[4,12,13] Temperature signals from thermocouples, kept in the melt, have been used to examine convection in the bottom or side heated metallic and semiconductor melt columns.[9,11,14–17] These studies have been concerned with either a stationary melt column or directional solidification with a planar liquid-solid interface. No such study is available for dendritic arrayed growth in a metallic alloy.

Convection in fluids is generally caused by unstable density gradients. Unstable density gradients can be caused by variations in composition and temperature. For example, upward directional solidification (with melt on top of the solid) of an alloy with a solute more dense than the solvent is both thermally and solutally stable, as is the case with the hypereutectic (tin concentration larger than eutectic) Pb-64.5 wt pct Sn. Solidification of that same alloy downward would be solutally and thermally unstable, the cool, solute-rich, heavier liquid near the solid-liquid interface creating the potential to naturally convect downward. The upward growth of an alloy with a solute less dense than the solvent, for example, the hypoeutectic (tin content less than eutectic) Pb-38 wt pct Sn, is thermally stable, but solutally unstable,[1,5] and may lead to thermosolutal convection. Solidification of this alloy downward would be thermally unstable and solutally stable. It is believed that convection in metals can be suppressed by application of a magnetic field, as has been demonstrated during plane front solidification of several electronic materials.[18] However, a direct examination of the influence of magnetic field on convection during dendritic growth of metallic alloys has not been carried out.

The main purpose of this study was (1) to study natural convection during dendritic arrayed growth of lead-rich, hypoeutectic, lead-tin alloys, both under thermally stable (melt on top and solid below) and thermally unstable (solid on top and melt below) conditions; (2) to examine the influence of magnetic field (applied transverse to the alloy growth direction) on convection; and (3) to correlate the observed temperature, convection, and macrosegregation. Since the solutal banding caused by convection is easier to observe during directional solidification of near eutectic alloy compositions, the tin-rich hypereutectic, Pb-64.5 wt pct Sn, alloy was also examined during downward growth.

II. EXPERIMENTAL PROCEDURE

About 24- to 30-cm-long Pb-Sn feed stock samples were obtained by induction melting a charge (lead and tin, 99.99 pct purity) under an argon atmosphere in a silica crucible and pushing the melt into evacuated silica tubes (0.7-cm i.d.) with the help of argon pressure. The silica tubes contained either two or four chromel-alumel thermocouples (TC1, TC2, TC3, and TC4: 0.01-cm diameter wires kept in closed-end silica capillaries, 0.06-cm o.d.) which were located along the sample length with a separation distance of about 1.5 cm. After sealing one end, the silica tubes containing these samples were evacuated and the top 15- to 20-cm length of the cast specimen was melted. Directional solidification was carried out in the high-temperature directional solidification furnace by raising (or lowering) the furnace assembly at various growth speeds (either 8 μm/s up, 8 μm/s down, or 0 μm/s) with respect to the stationary

H. SONG, Research Associate, and S.N. TEWARI, Professor, are with the Chemical Engineering Department, Cleveland State University, Cleveland, OH 44115. H.C. de GROH III, Materials Research Engineer, is with NASA–Lewis Research Center, Cleveland, OH 44135.

Manuscript submitted June 20, 1995.

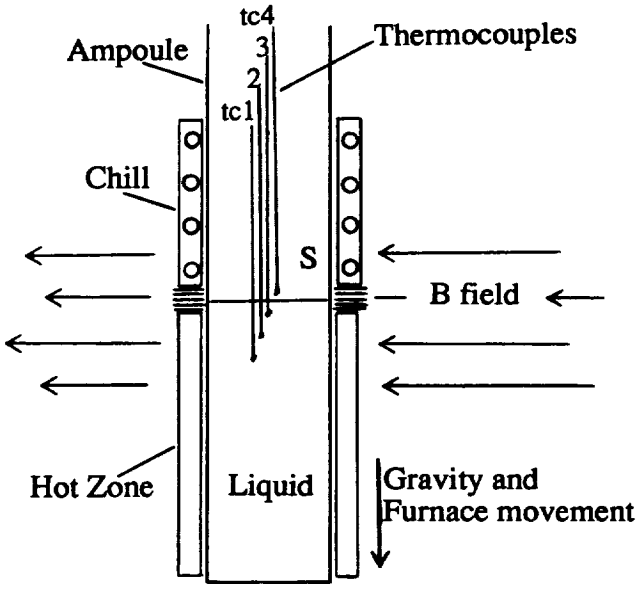

Fig. 1—Schematic of the high-temperature directional solidification furnace, showing the magnetic field perpendicular to the ampoule axis, the four thermocouples each spaced about 1.5 cm apart, with the ampoule fixed and the furnace moving.

sample. Figure 1 is a schematic of the furnace, with additional experimental details presented elsewhere.[1] The specimens were directionally solidified upward (melt on top of the solid) and downward (solid on top of the melt). Temperature profiles were recorded during translation of the furnace and also while maintaining the furnace assembly stationary at various locations. To examine different convective conditions, several hot zone temperatures were employed. The influence of 0 to 0.45 T magnetic field, applied transverse to the alloy growth direction, on the thermal profiles was examined. Ingot temperature measurements were analyzed using fast Fourier transformations (FFTs).

Longitudinal and transverse microstructures were examined in the unetched condition by standard optical metallography techniques. Two-millimeter-thick slices, machined along the length of the directionally solidified specimens, were analyzed for their tin content (C_s) by the "wet" chemistry technique atomic absorption spectroscopy to examine the longitudinal macrosegregation. The ratio of the distance solidified to the initial melt column length is taken as the fraction solidified (f_s).

A 1.25-cm-diameter, 11-cm-long, hypereutectic Pb-64.5 wt pct Sn ingot from a previous study is examined in more detail here.[19] This ingot, of composition close to the eutectic, yields a continuous examination of convective flow, aspect ratio, and Rayleigh number in the downward solidification mode. This ingot was solidified downward in the bulk undercooling furnace with two thermocouples in the melt, 9 cm apart, at a constant thermal gradient (4.6 K cm^{-1}) and cooling rate (7.7 K h^{-1}). Heaters at both ends were used to first induce an end-to-end temperature gradient. The temperatures of the two ends were then lowered at a constant rate. Thus, solidification was accomplished without movement of the furnace. It should be noted that although the global thermal gradient and cooling rate were constant, at certain times convective flows did cause local variations in the gradient and cooling rate. Wet chemical analysis at 0.5-cm intervals along the length of the ingot was used to obtain the composition variation. Details associated with this ingot can be found in Reference 19; however, of importance here is that the temperature gradient, G_l, was linear and imposed across the whole length of the ingot. Thus, as solidification progressed from the top down, the temperature difference between the solid-liquid interface and the hot bottom of the ingot (later defined as the temperature inversion, ΔT) continuously decreased. The height of the melt (later defined as h) also decreased. By contrast, ΔT and h were varied between Pb-38 wt pct Sn solidification runs by changing the hot zone temperature; however, once set, ΔT and h were constant for a particular Pb-38 wt pct Sn run.

III. RESULTS

A. *Convection under Destabilizing Thermal Profile*

The *in situ* thermal profiles, recorded during downward (solid on top and liquid below) directional solidification of hypoeutectic Pb-38 wt pct Sn at 0.8 μms^{-1} (Figure 2(a)), and the hypereutectic Pb-64.5 wt pct Sn ingot (Figure 2(b)) show extensive temperature fluctuations. Some temperature fluctuation is observed even in the mushy zone (mushy zone tips are assumed to be at the liquidus temperature of the bulk composition and the mushy zone base at the eutectic temperature). Such thermal fluctuations were not observed during upward (liquid on top and solid below) growth of the hypoeutectic Pb-38 wt pct Sn alloy, as shown in Figure 2(c).

The nature of thermal fluctuations during downward solidification was observed to depend upon the overall temperature inversion (ΔT) in the melt column and also on the thermal gradient at the particular longitudinal location or place in the gradient region being considered, termed the *local* thermal gradient in the melt (G_l). The temperature inversion refers to the unstable temperature difference between the hot liquid below, T_h, and the cool liquid above, T_{tip}, the solid-liquid interface. For the hypereutectic Pb-64.5 wt pct Sn ingot, ΔT varied continuously as solidification progressed and could be found easily by multiplying the melt height by the thermal gradient. For the Pb-38 wt pct Sn alloy, ΔT was varied by changing the hot zone temperature (where T_{tip} = 520 K was used). We will describe two typical hot zone temperatures. The hot zone temperature of 870 K corresponds to the more severe temperature inversion (ΔT = 350 K for a melt column length of 15 cm) and the hot zone temperature of 670 K to the less severe inversion (ΔT = 150 K for a melt column length of 12 cm).

1. *Influence of temperature inversion*

For the ΔT = 350 K inversion, the temperature fluctuations were observed to be random, as indicated by a typical thermal response (Figure 3(a), local melt temperature = 628 K) and its FFT (Figure 3(b)). For the ΔT = 150 K inversion, the fluctuations were not as random. Instead, there was a tendency for the signal to contain either one dominant frequency or several of its harmonics (Figure 5). Figures 4(a) and 5(a) show typical thermal responses from four thermocouples, located at varying distances from the tip of the mushy zone, and their FFTs (Figure 5(a)). The thermocouples, TC1 through TC3, located about 4, 2.5, and

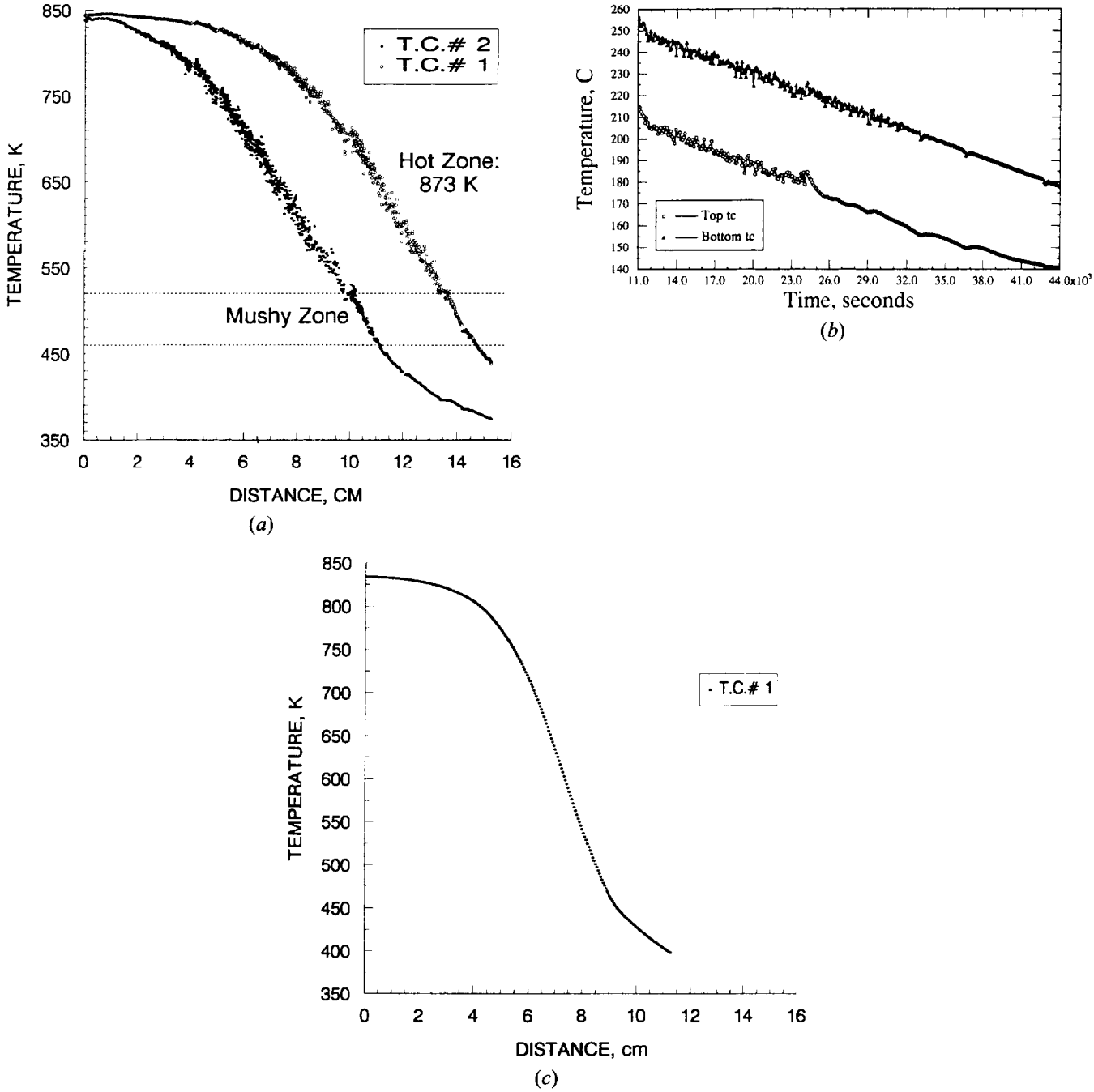

Fig. 2—*In situ* thermal profiles, recorded during directional solidification. (*a*) Downward growth of lead-rich (hypoeutectic) Pb-38 wt pct Sn (0.8 μm s^{-1}, hot zone temperature = 873 K, profiles from TC1 and TC2). (*b*) Downward growth of tin-rich (hypereutectic) Pb-64.5 wt pct Sn.[19] (*c*) Upward growth of hypoeutectic Pb-38 wt pct Sn (hot zone temperature = 873 K).

1 cm from the dendrite tips, appear to show one dominant frequency, about 0.06 Hz. Even the fourth thermocouple, TC4, which was located inside the mushy zone (about 0.5 cm from the dendrite tips), contains the 0.06 Hz signal, together with some other frequencies.

Figure 4(a) shows the temperature fluctuations, with the ΔT = 150 K inversion, on a broken temperature scale. All four thermocouples show the same dominant waveform with an approximately 16-second period. The temperature oscillations are shifted in time as indicated by the dashed lines in Figure 4(a); thus, it appears that a temperature rise (or drop) near the interface (TC4) travels along the length of the ingot down, finally being sensed by TC1 about 10 seconds later. The timing and phase shifting of these flows may shed light on the exact mechanics of the flow and will be discussed in more detail in a later section.

2. *Influence of local thermal gradient*

As shown in Figure 2(a), the magnitude of the temperature fluctuations is low in the hottest region of the melt, 830 to 840 K. Fluctuations increase with decreasing melt temperature, are maximum at about 650 K, and begin to decrease with further decreases in the local melt temperature. This is more clearly evident in Figure 6(a), which

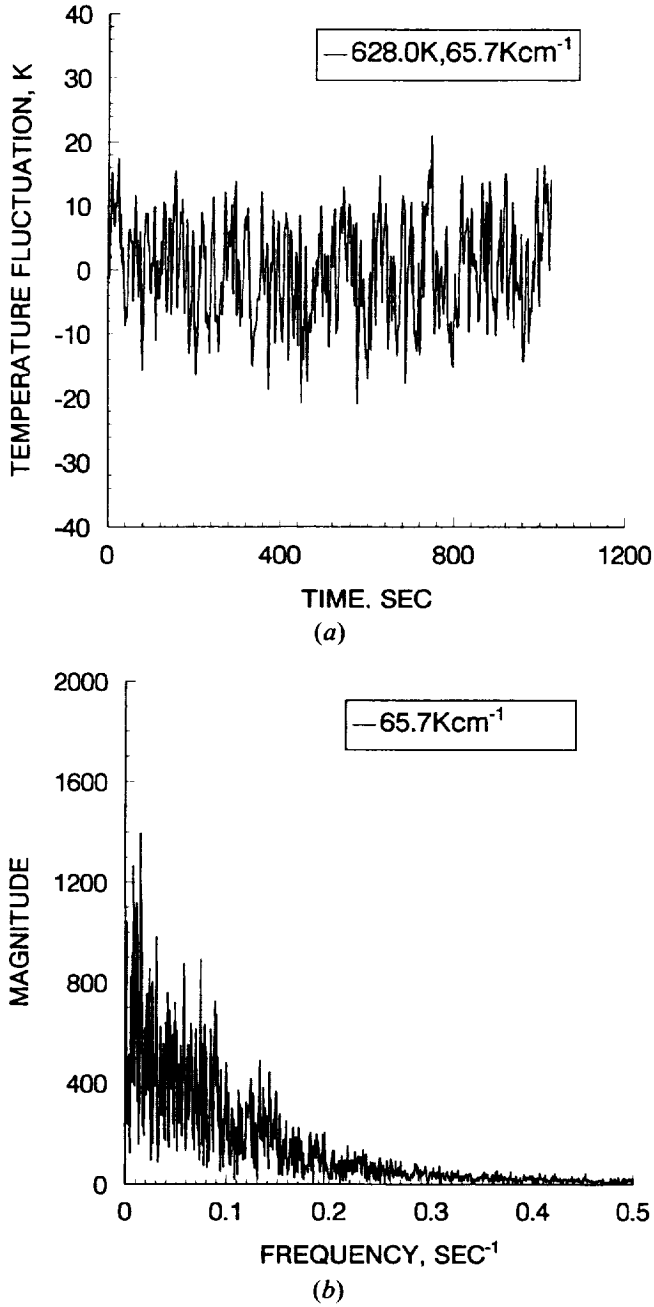

Fig. 3—Thermal response during downward growth of hypoeutectic Pb-38 wt pct Sn alloy (hot zone temperature = 873 K and ΔT = 350 K). (*a*) Random temperature fluctuations corresponding to the local melt temperature = 628 K. (*b*) The FFT of temperature fluctuations shown in (a).

combines temperature fluctuation data recorded by TC1 and TC2, shown as 4DI, while the furnace was held stationary at various locations, and uses one standard deviation from the mean to represent the magnitude of the temperature fluctuation. Data from several Pb-38 wt pct Sn alloy experiments have been included. The 4DI, 4EI, 4FI, and 4GI are for the more severe temperature inversion (ΔT = 350 K) and 4HI is for the less severe temperature inversion (ΔT = 150 K). The filled square symbol (4JI) is with the application of a 0.45 T magnetic field during growth with ΔT = 350 K. Dashed lines showing the location of the mushy zone are also included. These temperature fluctuation data have been replotted in Figure 6(b) as a function of G_l, the *local* thermal gradient in the melt.

The magnitude of the random temperature fluctuations, observed for the more severe temperature inversion in the melt, increases with increasing G_l. This trend is also observed for the oscillatory temperature fluctuations, observed during growth under less severe temperature inversion in the melt. However, for the same G_l, the temperature fluctuation is significantly greater when ΔT = 350 K than when ΔT = 150 K.

3. *Influence of transverse magnetic field*

The response of the temperature fluctuations to an applied magnetic field was observed to depend upon the extent of temperature inversion and the magnetic field strength.

a. *More severe temperature inversion*

Figure 7(a) shows how a typical temperature fluctuation responds to the application of the higher transverse magnetic field of 0.45 T for downward growth with ΔT = 350 K. With the application of the magnetic field, the random fluctuations initially decrease in magnitude and then pick up a constant amplitude and frequency. This behavior is not an artifact of the magnetic field, as verified by the thermocouples kept in the solid portion of the specimen. It should also be mentioned here that the application of magnetic field does not produce any temperature oscillations for the thermally stable and solutally unstable growth conditions (melt on the top and solid below).

The temperature fluctuations which were random became oscillatory with the application of the magnetic field, containing either one dominant frequency or several harmonics. The fluctuations with initially larger amplitude usually show multiple harmonics, as shown by a typical FFT (Figure 7(b)). This signal contains harmonics of 0.11 Hz. Application of the magnetic field reduces the magnitude of the temperature oscillation; for example, a $\pm$2.1 K fluctuation with the field *vs* $\pm$7 K without (Figure 6(a), comparing 4JI and 4DI at about 700 K). The small ($\pm$0.47 K) amplitude fluctuations present, for example, near the base of the dendrites, which were random in the absence of magnetic field, became sinusoidal (containing one dominant frequency), as seen by a typical FFT (Figure 7(c)). However, the maximum available transverse magnetic field of 0.45 T was insufficient to completely suppress the convection and temperature fluctuations under these conditions.

b. *Less severe temperature inversion*

The temperature fluctuations in the presence of less severe temperature inversion in the melt (ΔT = 150 K) were not random but had an oscillatory tendency (Figures 4(a) and 5). In the presence of a magnetic field, these signals remained oscillatory, but they became significantly less noisy as seen by comparing Figures 4(a) through (c). This is also seen by comparing the FFTs of the thermal responses of the four thermocouples in the presence and absence of a magnetic field (Figures 5(a) through (c)). In the presence of 0.05 T magnetic field, the three temperature profiles, TC1 through TC3, recorded at 4 cm (653 K), 2.5 cm (611 K), and 1 cm (563 K) from the dendrite tips, and TC4, recorded in the mushy zone (0.5 cm away from the dendrite tips), showed oscillatory signals with the same 0.06 Hz frequency. The temperature fluctuations, as char-

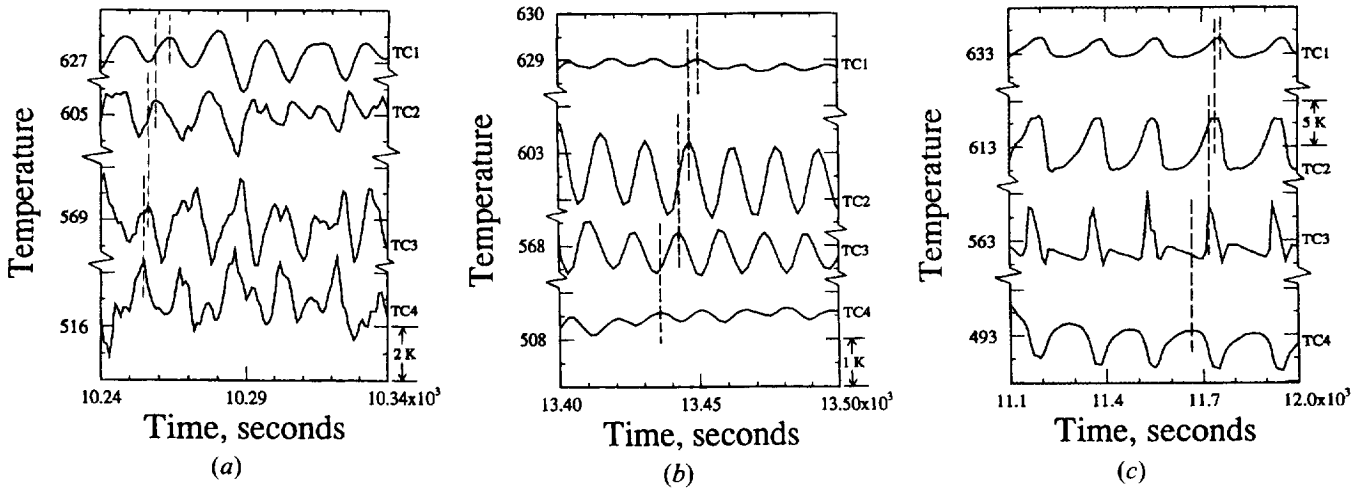

Fig. 4—Thermal response, shown on a broken temperature axis, during downward growth of hypoeutectic Pb-38 wt pct Sn (hot zone temperature = 673 K and ΔT = 150 K) recorded by four thermocouples separated by 1.5 cm. TC4 is just inside the mushy zone and on top, with TC3, 2, and 1 below and further out in the gradient region. Phase shifts among thermocouples are shown by the dashed lines: (*a*) no magnetic field applied with average phase shift between TC4 and 3 (P_{4-3}) of 1.9 s, $P_{3,2}$ = 3.1 s, and P_{2-1} = 4.8 s; (*b*) with 0.05 T magnetic field applied, $P_{4,3}$ = 6.0 s, $P_{3,2}$ = 4.6 s, and $P_{2,1}$ = 4.1 s; and (*c*) with 0.15 T magnetic field, $P_{4,3}$ = 67 s, $P_{3,2}$ = 14 s, and $P_{2,1}$ = 13 s.

acterized by the standard deviation of temperature, with ΔT = 150 K, were ± 0.79 K with no magnetic field, ± 0.49 K at 0.05 T, and ± 1.54 K with the 0.15 T field. At moderate magnetic field, 0.15 T, the 0.06 Hz signal vanished, yielding a slower cyclic signal with 0.005 Hz frequency (Figure 4(c) and 5(c)). Interestingly, the temperature waveform changes from a predominantly sinusoidal wave at 0.05 T to a pulsed wave when the magnetic field is 0.15 T. This change in the waveform makes comparison of the temperature fluctuations through the standard deviation from the mean less reliable, the waveform at the 0.15 T field being better characterized by the approximately +5.5 K pulse rising from a baseline (Figure 4(c)). This type of pulsed flow is indicative of the flow which might cause composition striations during solidification. It should be mentioned that we closely examined the FFTs of the lower magnetic fields (zero, Figure 5(a) and 0.05 T (Figure 5 (b)) and found no 0.005 Hz peak. As shown in Figure 5, the amplitude of the FFT power spectrum for the new 0.005 Hz signal was an order of magnitude larger than that observed at 0.05 T, or without the application of the magnetic field, showing the purity and strength of this pulsed flow.

B. *Microstructure*

Figure 8 shows typical microstructures observed for the Pb-38 wt pct Sn alloy directionally solidified: (a) upward and (c) downward. For upward growth, the distribution of primary dendrites was uniform across the entire specimen cross section, except for occasional channel segregates observed near the specimen periphery, which were continuous along the length of the directionally solidified specimens.[1] The length of the primary dendrites was uniform across the entire mushy zone, as shown in the longitudinal microstructure at the quenched liquid-solid interface (Figure 8(a)). The uniform distribution of primary dendrites was also evident on the transverse section, as shown in Figure 8(b). For downward growth, the length of the primary dendrites in the mushy zone was not uniform, as shown in the longitudinal microstructure at the quenched liquid-solid interface (Figure 8(c)). Several dendrite clusters can be observed to protrude ahead of their neighboring dendrites. This results in a very nonuniform distribution of primary dendrites in the directionally solidified portion of the specimen. This is evident from Figure 8(d), which shows microstructures from two regions on the same transverse section. Isolated pockets of tin-rich regions were observed on the specimen cross section. However, these were not continuous along the length of the directionally solidified specimens, as was the case with the previously described channel segregates. Such dendrite clustering has been observed in hypoeutectic Pb-Au[7] and Al-Cu alloys,[20] solidified upward, and Pb-40 wt pct Sn, solidified downward.[6]

Figure 9 shows the macro- and microstructure along the length of the hypereutectic Pb-64.5 wt pct Sn alloy ingot solidified downward.[19] Bands of irregular convex and concave striations were observed in the top 5-cm portion of the sample (length of the initial melt column = 11 cm). The top 4.4 cm of this region contained tin-rich dendrites (and eutectic), and the rest contained aligned eutectic only. The structure of the Sn-rich ingot evolves from dendritic to eutectic because of Pb enrichment of the liquid (due to primary Sn dendrite solidification) and the movement, as expected, of the liquid and solid compositions along the liquidus and solidus until the eutectic is reached. Irregular striations ended abruptly at a melt column height (h) of 6 cm and were replaced by regular striations with a characteristic frequency of 0.028 Hz. The microstructure in this region mostly consisted of aligned lead-tin eutectic. For the melt column less than 4.4 cm, no striations were observed, and the microstructure consisted of aligned eutectic.

C. *Macrosegregation*

Macrosegregation along the length of the directionally solidified hypoeutectic Pb-38 wt pct Sn ingot is shown in Figure 10(a), where variation in the solute content (C_s/C_0) is plotted as a function of fraction solidified. The open symbols correspond to the directionally solidified portion and the filled symbols to the quenched melt. This alloy, when

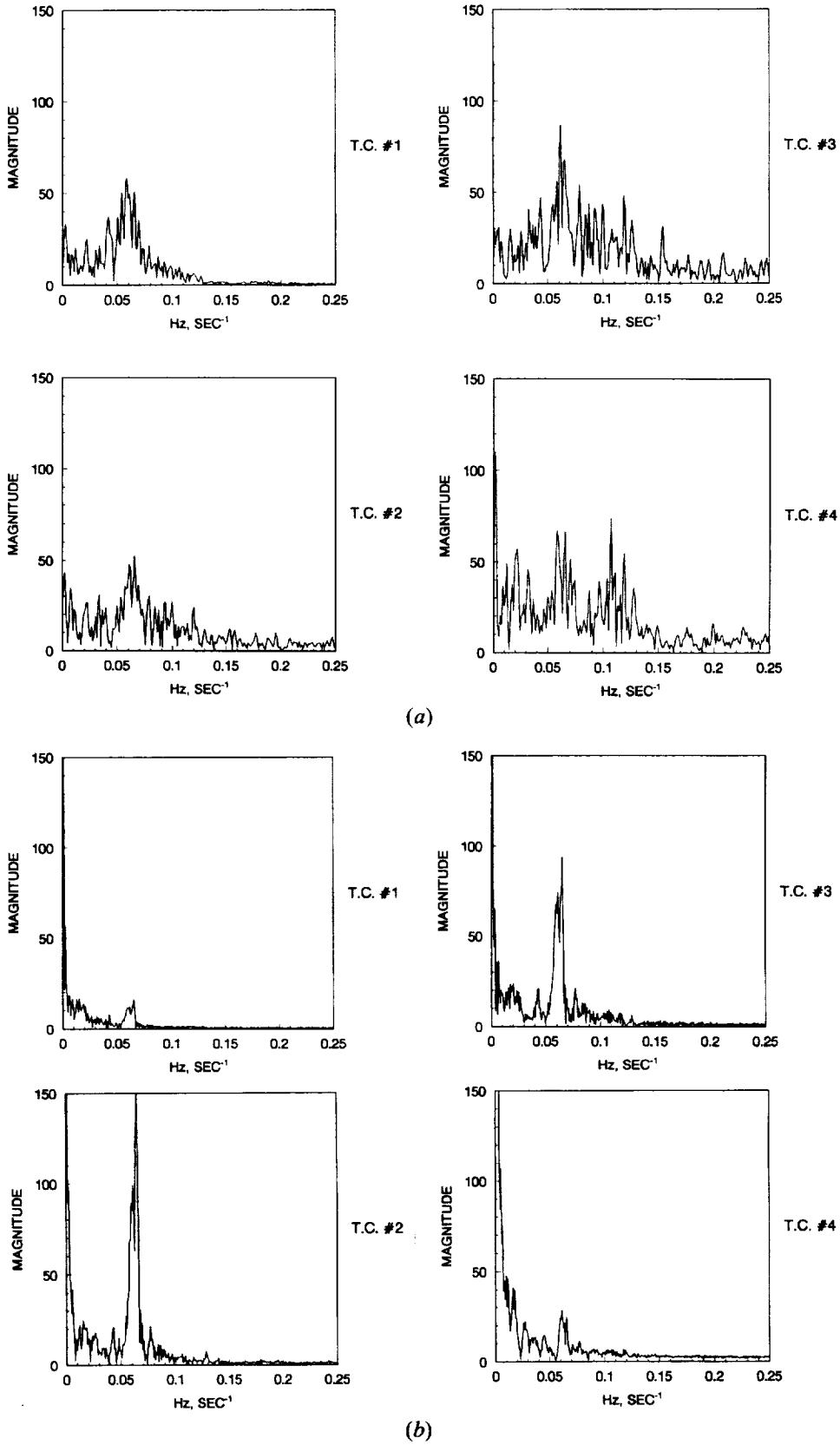

Fig. 5—FFTs of temperature fluctuations measured at different locations during downward growth, ΔT = 150 K: (*a*) no magnetic field, temperatures shown in Fig. 4(a); (*b*) with 0.05 T magnetic field applied, temperatures shown in Fig. 4(b); (*c*) with 0.15 T field, temperatures of Fig. 4(c).

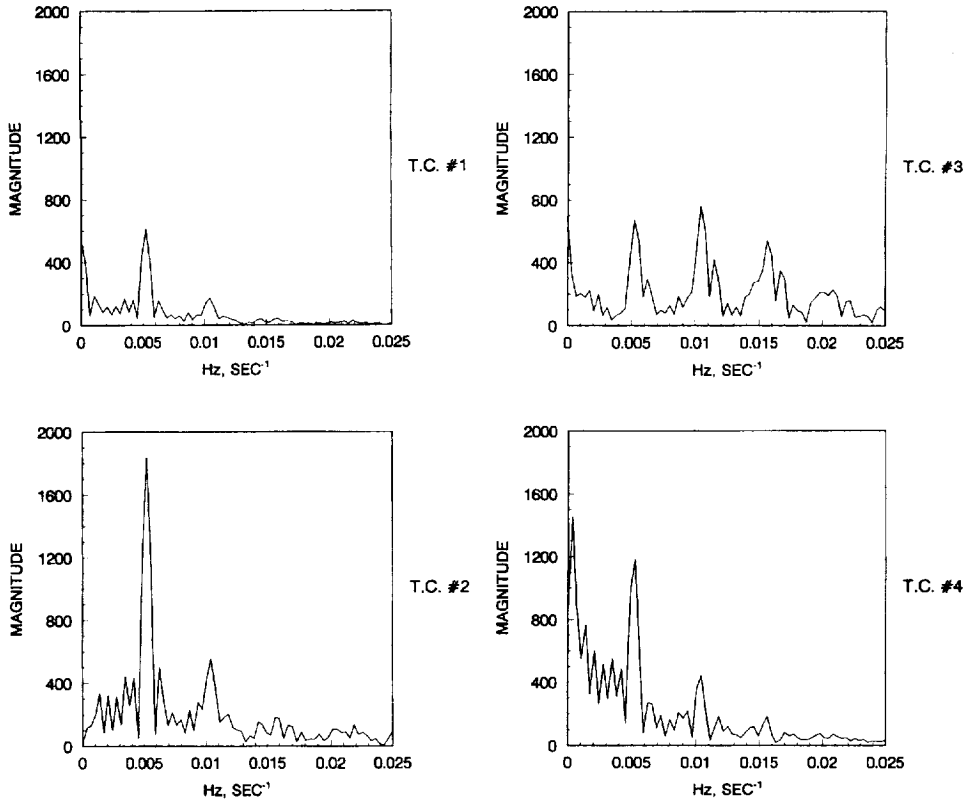

(*c*)

Fig. 5—(*Continued*) FFTs of temperature fluctuations measured at different locations during downward growth, ΔT = 150 K: (*a*) no magnetic field, temperatures shown in Fig. 4(a); (*b*) with 0.05 T magnetic field applied, temperatures shown in Fig. 4(b); (*c*) with 0.15 T field, temperatures of Fig. 4(c).

directionally solidified upward,[1] showed a systematic longitudinal macrosegregation (triangular symbols in Figure 10 (a)). Notice the significantly higher tin content of the quenched melt as compared to C_0. For downward growth, there is large scatter in the tin content along the directionally solidified length; however, there is no systematic longitudinal macrosegregation. Notice that the tin content of the quenched melt portion is nearly equal to C_0. The downward grown hypereutectic Pb-64.5 wt pct Sn ingot, on the other hand, does show longitudinal macrosegregation (Figure 10(b)).

IV. DISCUSSION

A. *Correlation between Convection and Macrosegregation*

Let us examine typical specimen configurations and the resulting temperature, composition, and melt density profiles during directional solidification of a binary alloy (Figure 11(a)). The composition of the melt increases from C_0, the original solute content of the bulk melt, to C_l at the dendrite tips and to C_E, the eutectic composition, at the base of the dendrites. The increasing solute content in the melt may decrease its density (hypoeutectic Pb-38 wt pct Sn) or increase it (hypereutectic Pb-64.5 wt pct Sn[19] or hypoeutectic Pb-8 wt pct Au[7]).

During downward growth (Figure 11(b)), the temperature profile is expected to be destabilizing, providing a driving force for natural convection for the Pb-38 wt pct Sn alloy. The solutal profile, however, would be stabilizing within the mushy zone and in the immediate vicinity of the dendrite tips. One would, therefore, expect natural convection to occur in the bulk melt but not in the mushy zone. During upward growth of hypoeutectic Pb-38 wt pct Sn (Figure 11(c)), the temperature profile would be stabilizing against natural convection, but the composition profile would be destabilizing, both within the mushy zone and in the immediate vicinity of the dendrite tips. One would, therefore, expect natural convection to occur within the mushy zone. Upward growth of the hypereutectic Pb-64.5 wt pct Sn or Pb-8 wt pct Au alloy, with melt on top and solid below (Figure 11(d)), would produce stabilizing thermal and solutal profiles in the bulk melt and in the mushy zone. Convection would, therefore, not be expected. Downward growth of the hypereutectic Pb-64.5 wt pct Sn (Figure 11(e)), however, would produce unstable thermal and solutal profiles in the bulk melt and also in the mushy zone. One would, therefore, expect convection to occur.

It is interesting to note that despite extensive convection, as evidenced by the thermal fluctuations (Figure 2(a)), the hypoeutectic Pb-38 wt pct Sn alloy, when directionally solidified downward (Figure 11(b)), did not show any longitudinal macrosegregation (Figure 10(a)). However, upward growth of this alloy (Figure 11(c)) resulted in extensive longitudinal macrosegregation (Figure 10(a)), even though no temperature fluctuations were observed (Figure 2(c)). The longitudinal macrosegregation is indirect evidence of convection, but temperature fluctuations have never been observed during our intensive examination of upward growth

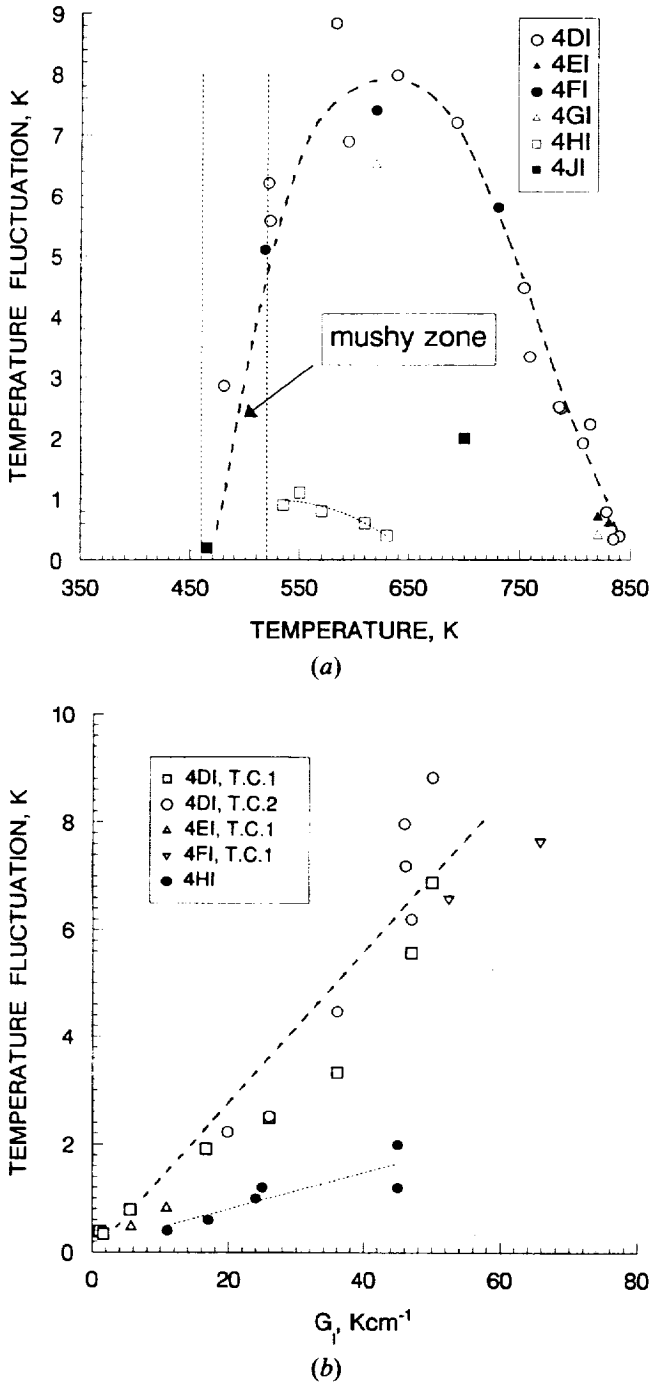

Fig. 6—Temperature fluctuations as a function of (*a*) sample temperature and (*b*) local thermal gradient. 4DI, 4EI, 4FI, and 4GI were for ΔT = 350 K, 4HI used ΔT = 150 K, and 4JI was for ΔT = 350 K and a magnetic field of 0.45 T.

of hypoeutectic Pb-Sn alloys (C_0 varying from 10 to 58 wt pct tin, growth speed varying from 0.3 to 66 μm s^{-1}, and the hot zone temperature varying from 570 to 1070 K).

Macrosegregation along the length of the directionally solidified samples can result only in the presence of significant mixing between the interdendritic liquid and the bulk melt. Convection in the bulk melt, alone, cannot produce longitudinal macrosegregation. This is demonstrated by the absence of longitudinal macrosegregation for the downward growth of the hypoeutectic Pb-38 wt pct Sn, where because of the stabilizing conditions present in the interdendritic melt (Figure 11(b)), the convection in the bulk melt is not able to penetrate significantly into the mushy zone. Even vigorous convection, produced by stirring the bulk melt, has been found to be ineffective in producing longitudinal macrosegregation during an upward dendritic arrayed growth of Sn-2.5 wt pct Ag (schematic Figure 11(d)), due to the stabilizing density profile within the interdendritic melt.[3] For cases such as these, where interdendritic permeabilities are low, longitudinal macrosegregation is produced only when the interdendritic density profile is destabilizing. This is the case with the hypoeutectic Pb-38 wt pct Sn, directionally solidified upward (schematic in Figure 11(c)), where convection occurred, possibly as fluid "plumes" from the mushy zone rising into the bulk melt, as has been observed during dendritic growth of a transparent alloy, NH4Cl + water.[12] The flow, however, is laminar. Therefore, any location in such a convection cell would experience a constant temperature as a function of time, and no temperature fluctuation would be recorded, as is experimentally observed. Application of a transverse magnetic field would introduce an anisotropy in the flow, because it would reduce the velocity of the fluid flowing normal to the applied field. This has been observed to distort the mushy zone morphology near the tips of the dendrite array, especially for the growth conditions with large driving force for convective instability.[21] However, this does not affect the extent of mixing between the interdendritic and bulk melts, as evidenced by the identical longitudinal macrosegregation profiles observed in the specimens, grown with and without the application of a transverse magnetic field.[21] The growth condition, schematically shown in Figure 11(e), also produces longitudinal macrosegregation (Figure 10(b)) because the convection from the bulk melt is able to penetrate deep into the mushy zone due to the destabilizing interdendritic density profile. This has also been observed in Sn-31 pct Pb and Pb-8 pct Au alloys.[6]

For growth conditions, schematically shown in Figure 11(b) (Pb-38 wt pct Sn, solidified downward) and Figure 11(d) (Pb-8 wt pct Au[7] or hypoeutectic Al-Cu alloy,[22] solidified upward), no longitudinal macrosegregation is produced. Instead, as shown in Figure 8(c), a transverse macrosegregation, in the form of dendrite clustering (dendrite steepling), is produced. The length of the primary dendrites is not constant in the entire mushy zone. In the most severe manifestation of such a transverse macrosegregation, portions of the mushy zone do not contain any primary dendrites, even at the base of the mushy zone. The convection, responsible for such transverse macrosegregation, is confined to the immediate vicinity of the dendrite tips. As originally pointed out by Burden *et al.*[22] for hypoeutectic Al-Cu alloys, dendrite steepling commences when one primary dendrite in the dendritic array accidently leads (or lags) its neighbors in growth. As schematically shown by the dotted line profile of a leading dendrite in Figure 11(d), this suppresses the growth of the neighboring dendrites, which are forced to grow into a region made solute rich, because of the solute rejected into the melt around the tip of the leading dendrite. The solute-rich heavier melt flows down, further suppressing growth of other neighboring dendrites, and causes a distorted liquid-solid interface at the dendrite tips. A similar phenomenon would be expected to

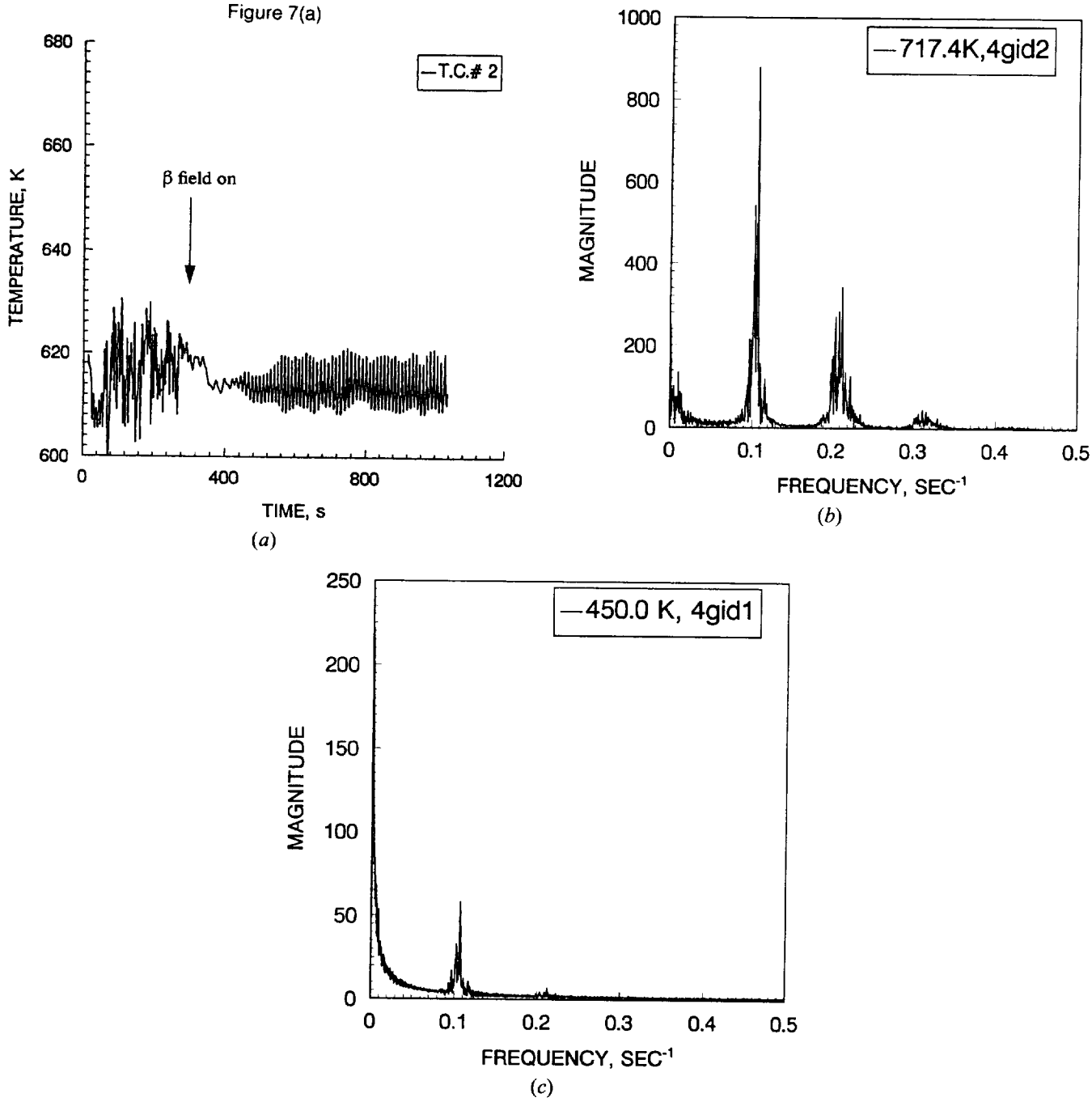

Fig. 7—Response of the temperature fluctuations, present during downward growth, to the application of a transverse magnetic field with a hot zone temperature of 870 K (ΔT = 350 K). (*a*) Temperature fluctuations without the field are on the left side and those with the field are toward the right side of the figure. (*b*) Large magnitude random fluctuations are oscillatory, containing multiple harmonics after application of a transverse magnetic field. (*c*) Small magnitude ($\pm$0.47 K) random fluctuations near the base of the mushy zone become cyclic, with a single characteristic frequency, in the presence of magnetic field.

occur during downward growth of hypoeutectic Pb-38 wt pct Sn (Figure 11(b)), as pointed out by Verhoeven *et al.*[6] As shown by the dotted line profile of a leading dendrite in Figure 11(b), the lighter, solute-rich melt would flow upward from near the tip of the leading dendrite and suppress the growth of its neighboring dendrites. This would also result in dendrite steepling, a nonuniform dendrite length in the mushy zone.

The structure of the Pb-38 wt pct Sn ingot indicates that some dendrites are highly fragmented and in regions of low solid fraction. Free, unattached dendrites in these regions are able to sink, thereby moving into hot liquid and remelting. These phenomena would mitigate solute transported from the region of the dendrite tips and macrosegregation.

B. *Temperature Oscillations during Downward Growth*

Convection due to the destabilizing thermal gradient has been examined in vertical columns of liquid metals[14,15]

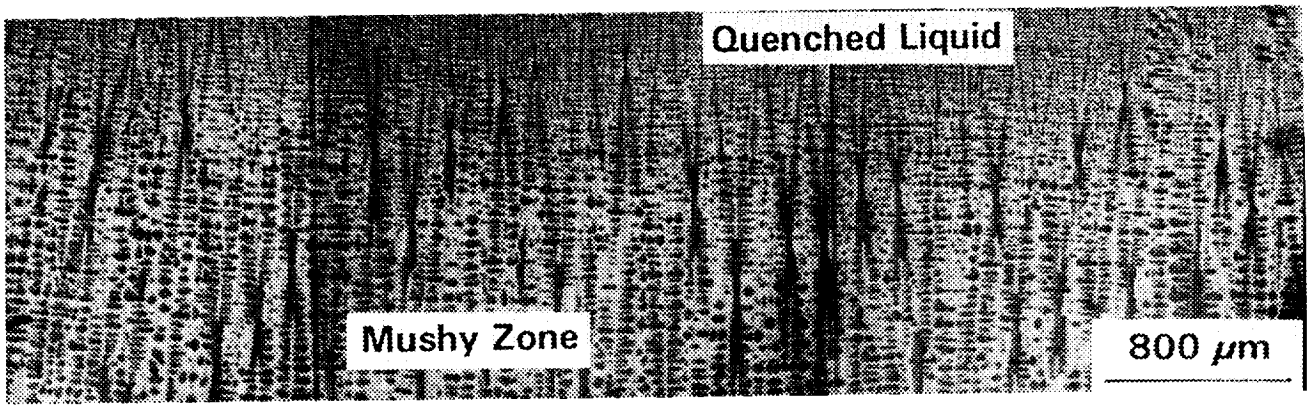

(*a*)

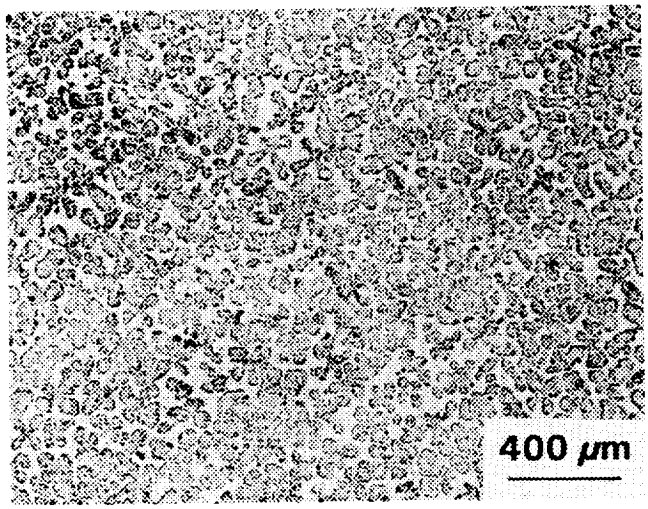

(*b*)

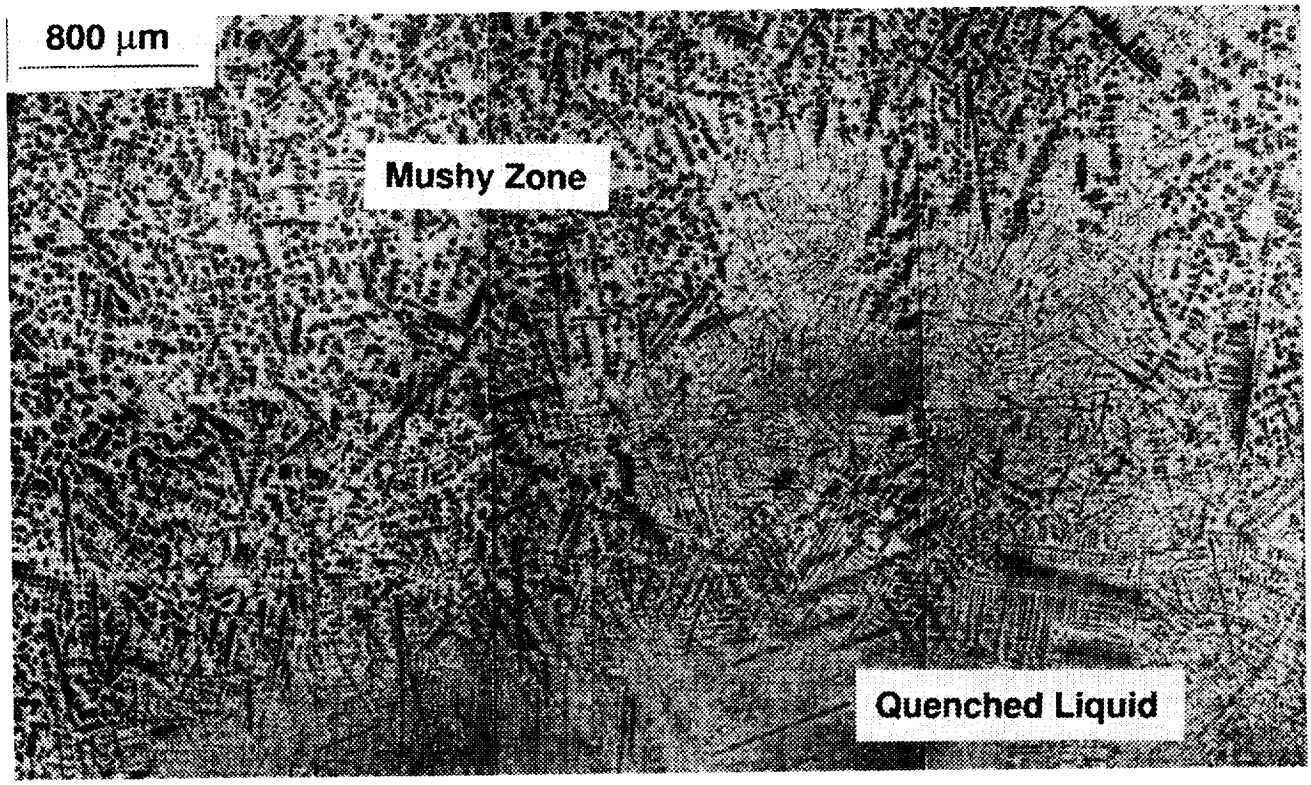

(*c*)

Fig. 8—Typical transverse and longitudinal microstructures of directionally solidified hypoeutectic Pb-38 wt pct Sn alloy. (*a*) Longitudinal section at the quenched liquid-solid interface: solidified upward. (*b*) Transverse: solidified upward. (*c*) Longitudinal section at the quenched liquid-solid interface: solidified downward. (*d*) Two typical microstructures from the same transverse section: solidified downward.

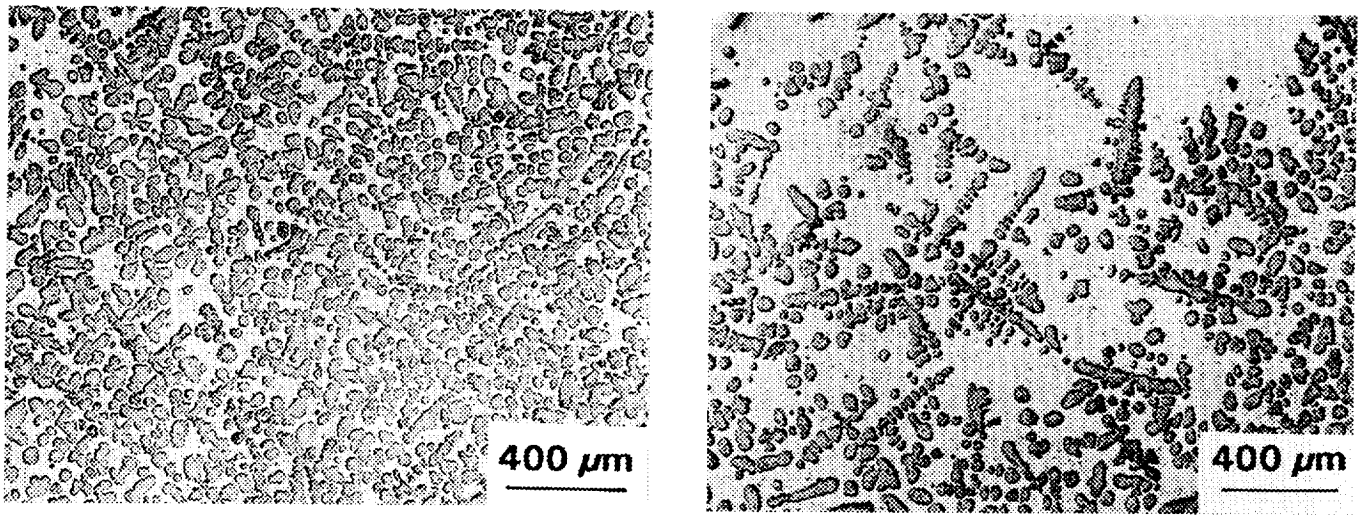

(d_1) (d_2)

Fig. 8—(*Continued*) Typical transverse and longitudinal microstructures of directionally solidified hypoeutectic Pb-38 wt pct Sn alloy. (*a*) Longitudinal section at the quenched liquid-solid interface: solidified upward. (*b*) Transverse: solidified upward. (*c*) Longitudinal section at the quenched liquid-solid interface: solidified downward. (*d*) Two typical microstructures from the same transverse section: solidified downward.

(mercury and gallium), semiconductors[11,17] (InSb), and water,[16] as well as in gases.[23] It has been observed that the nature of the convection depends upon three factors: (1) the Rayleigh number ($Ra = g\beta \Delta T h^3/\kappa\nu$, where g is the acceleration due to gravity, β is the volumetric thermal expansion coefficient, $\Delta T = T_{hot} - T_{tip}$ is the temperature inversion over a melt height, h, κ is the thermal diffusivity, and ν is the kinematic viscosity); (2) the Prandtl number: ν/κ; and (3) the aspect ratio h/d (d is the inner diameter of the cylinder). Figure 12, from Reference 17, shows the relationship between the Rayleigh number and aspect ratio for the onset of various convective modes. The broken curve, at the bottom, corresponds to the onset of steady-state convection at a critical Rayleigh number (Ra_{c1}). Here, the temperatures inside the melt are steady. A transition to unsteady, time-periodic flow occurs at a higher Rayleigh number (Ra_{c2}) (indicated by the solid curve), which results in oscillatory temperature fluctuations. At a still higher Rayleigh number (Ra_{c3}) (indicated by the dotted curve at the top), a transition from time-periodic to unsteady turbulent flow occurs, which causes random temperature fluctuations inside the melt. The longitudinal microstructure of the downward solidified hypereutectic Pb-64.5 wt pct Sn alloy (Figure 9) is in agreement with this behavior. For this specimen, the thermal gradient (G_l) remained constant while the liquid column height, h, and the aspect ratio of the melt column, h/d, decreased as solidification progressed. The unstable temperature inversion, ΔT, equal to the product of $G_l \times h$ for the Pb-64.5 wt pct Sn ingot, also decreased. The Rayleigh number was therefore continuously decreased. The striations in Figure 9, changing from random to time periodic and finally being absent, are indicators of the nature of convection in the melt. The striations are due to changes in growth speed and composition as a result of the solid-liquid interface coming in contact with a hot or cold fluid stream. A sudden increase in the growth speed causes additional solute to be rejected, producing a lead-rich region in the melt ahead of the liquid-solid interface, causing the observed striations in the solidified microstructure. The random and time-periodic striations indicate, respectively, unsteady turbulent and time-periodic flows. The experimentally observed critical Rayleigh numbers for these transitions and the corresponding aspect ratios, indicated in Figure 12 ($Ra_{c2} = 3.8 \times 10^5$ at $h/d = 3.53$ and $Ra_{c3} = 1.3 \times 10^6$ at $h/d = 4.80$, with Pb-Sn physical properties taken from References 25 and 26), are in good agreement with previous work in low Prandtl number ($Pr \approx 0.02$) fluids. It is interesting to note that the observed frequency of the unsteady time-periodic flow, 0.028 Hz ($h/d = 3.5$), is also in agreement with the value of 0.027 Hz, reported for Te-doped GaSb, at the similar $h/d = 2.7$.[17] Similar regions of turbulence, periodic flow, and steady thermal conditions were reported by Kim *et al.*[11] We observed (Figure 5(c)), as have others,[24] turbulence to develop over a series of steps indicated by period-doubling bifurcations (the presence of harmonics of the primary frequency) in the FFT of temperature.

Because the temperature profiles during downward growth of hypoeutectic Pb-38 wt pct Sn alloy were not linear (Figure 2(a)), Rayleigh numbers are difficult to determine. However, reasonable Ra can be determined by taking the temperature difference between the hot zone and the dendrite tips to be equal to ΔT and taking h to be the distance over which this temperature change would have occurred had the observed maximum temperature gradient been constant between the interface (dendrite tips at the liquidus temperature) and the hot zone. Thus, ΔT and h were constant for a particular Pb-38 wt pct Sn run. The Rayleigh numbers for the previously described two growth conditions, less severe temperature inversion ($\Delta T = 150$ K) and more severe temperature inversion ($\Delta T = 350$ K), are, respectively, 1.2×10^6 ($h/d = 4.8$) and 2.7×10^7 ($h/d = 10$). The high Rayleigh number, 2.7×10^7, lies in the unsteady turbulent region (Figure 12). One would therefore expect random thermal fluctuations, as were experimentally observed (Figure 3). The lower Rayleigh number, 1.2×10^6, closer to the time-periodic region and below Ra_{c3}, as determined in the Pb-64.5 wt pct Sn sample, suggests that

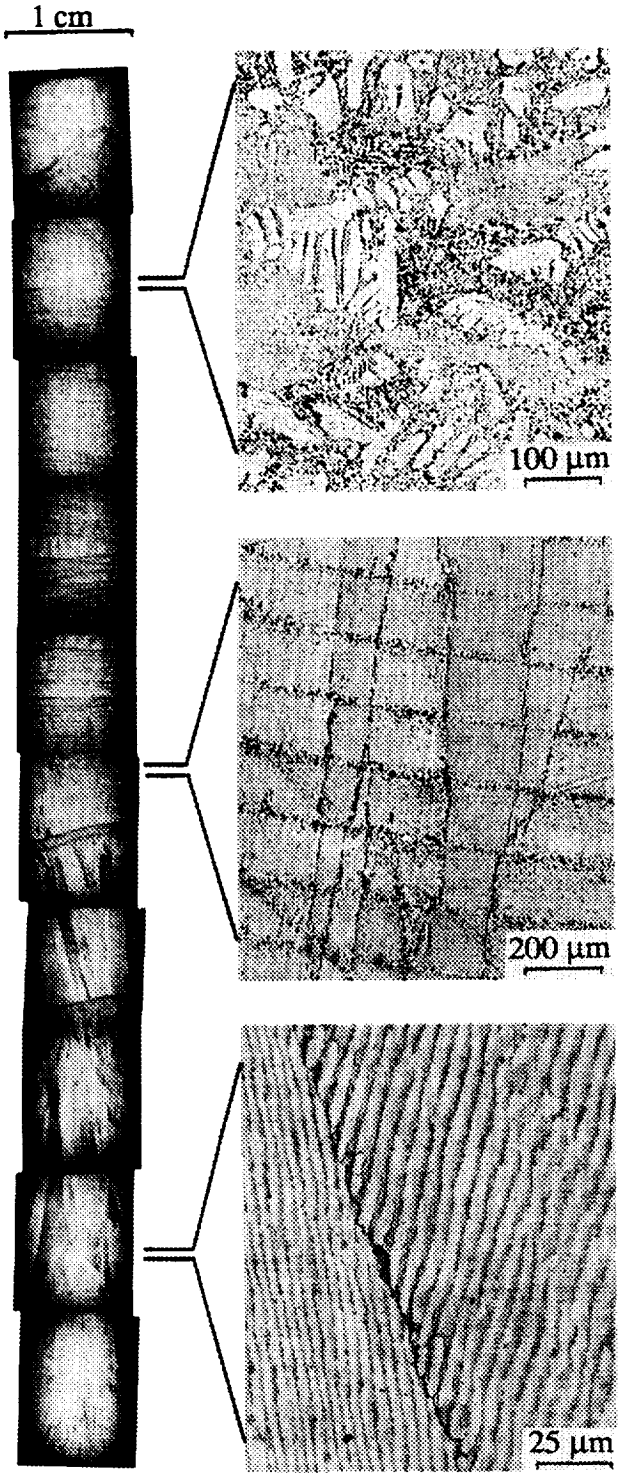

Fig. 9—Macro- and microstructure along a hypereutectic Pb-64.5 wt pct Sn ingot solidified downward[19] with irregular striations in the upper portion of the sample, showing evidence of turbulent flows; regular, evenly spaced striations near the center, indicating the presence of cyclic or pulsing flows; and no disturbances in the lower portion of the ingot.

time-periodic temperature variations should be present. This is in agreement with the observed behavior; the FFT of the temperature signals tends to contain one dominant frequency (Figure 5). In particular, at $\Delta T = 150$ K, with the application of the 0.05 and 0.15 T fields, the flow

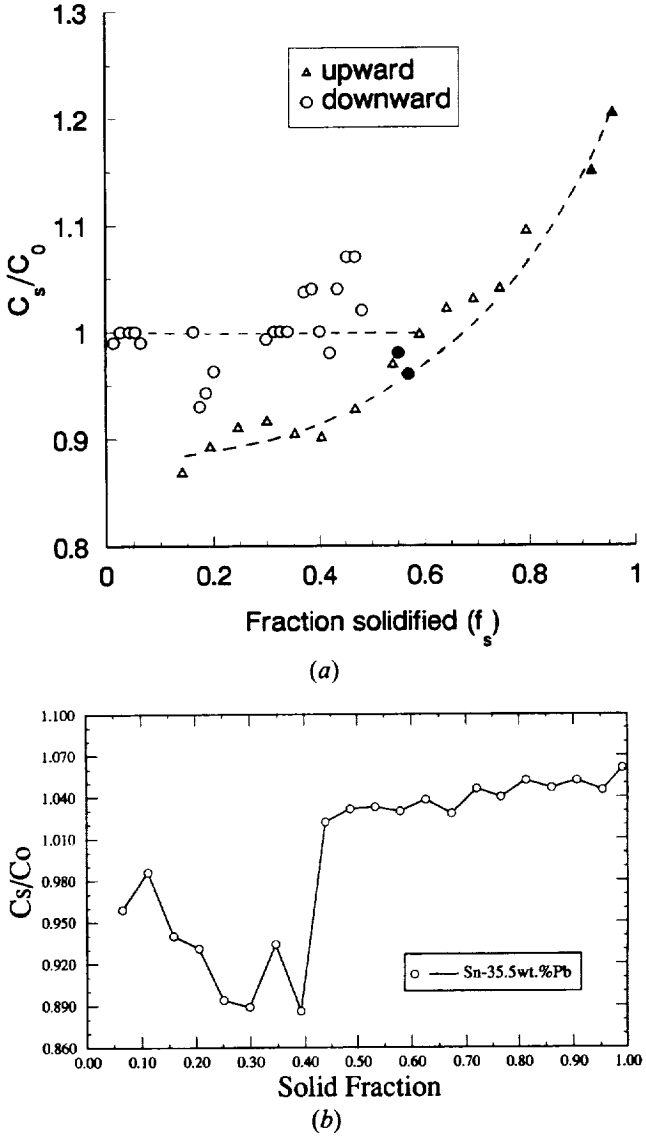

Fig. 10—Variation in the solute content (C/C_0) as a function of fraction solidified. The open symbols correspond to the directionally solidified portion and the filled symbols to the quenched melt: (*a*) Lead-rich, hypoeutectic, Pb-38 wt pct Sn solidified upward and downward; and (*b*) Tin-rich, hypereutectic, Pb-64.5 wt pct Sn, solidified downward.[19]

clearly moved toward sinusoidal and pulsed time-periodic flows characteristic of lower Ra.

Several possibilities have been suggested in the literature to explain the previously described time-periodic temperature oscillations. Rotation of flow axis around the container axis,[27] flow *via* three-dimensional spirals rotating about the axis of suboscillatory flow,[23] pulsed flow, flow in the same direction with varying speed,[14] and periodic change of flow configuration of a double roll[16] have been suggested as possible flow configurations responsible for the time-periodic temperature fluctuations observed at Ra above Ra_{c2}. Although temperature measurements provide evidence of time-periodic and turbulent convection, the corresponding flow patterns have only been observed in high Prandtl number transparent fluids (water: Pr ≈ 6.7[16] and gases: Pr ≈ 1[27]). For water,[16] the single cellular, nonaxisymmetric, steady-state flow, occurring at the onset of convection, generated two additional cells at the top and bottom corners of

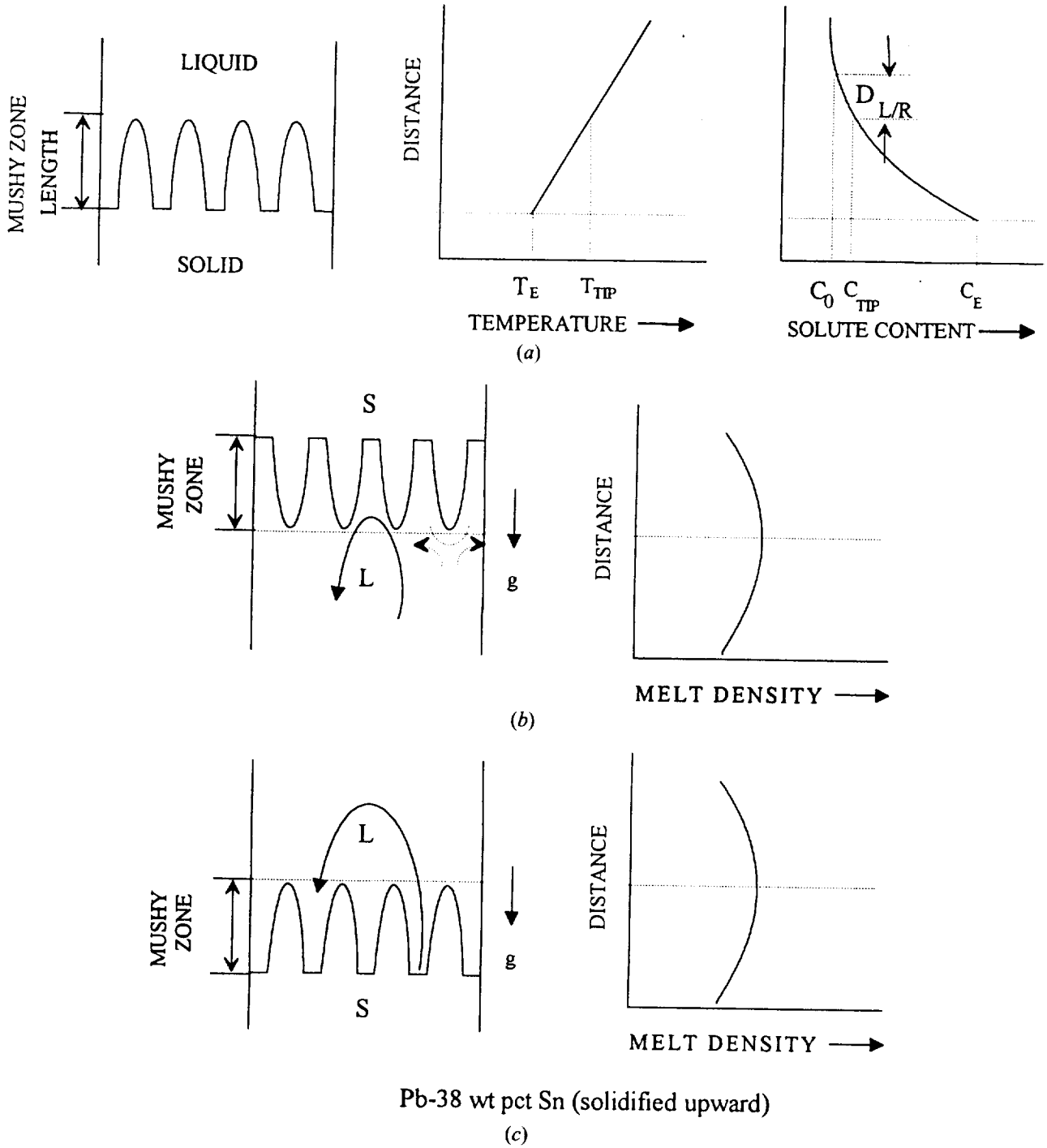

Fig. 11—(*a*) Typical specimen configurations and the resulting temperature, composition, and melt density profiles during directional solidification of a binary alloy, (*b*) Pb-38 wt pct Sn (solidified downward); (*c*) Pb-38 wt pct Sn (solidified upward); (*d*) Pb-8 wt pct Au (solidified upward); and (*e*) Pb-8 wt pct Au (solidified downward).

the major cell at a higher Rayleigh number. At a still higher Rayleigh number, a double roll time periodic flow configuration resulted which was associated with the unsteady time-periodic temperature oscillations. Though not definitively conclusive, our consideration of the present data indicates that the temperature oscillations are due to variations in flow velocity mostly along the ampoule axis. The presence of the fluid moving rapidly down along the axis is indicated by the consistent phase shift among the temperature readings of TC1, 2, 3, and 4. These time shifts are shown in Figure 4, as are the change in the phase shifts as the magnetic field is imposed. The phase shifts can be used to determine the movement of the longitudinal wave and its velocity, which is an indication of fluid flow velocities. The velocity of the wave (the axial flow) is simply the distance between the thermocouples divided by the duration of the phase shift. Averaging the shifts of three waves, using only the shift between TC2 and 3, the axial wave velocities for $\Delta T = 150$ K, with zero, 0.05, and 0.15 T fields, were 4.8×10^{-3}, 3.3×10^{-3}, and 1.1×10^{-3} m/s,

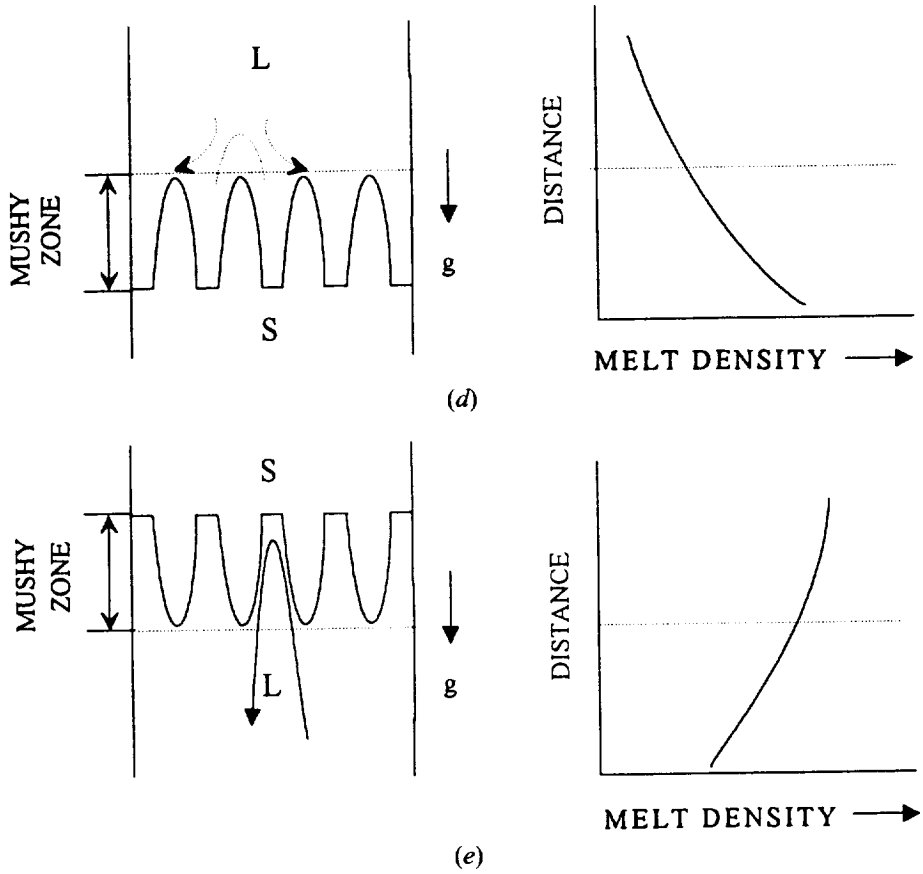

Fig. 11—(*Continued*) (*a*) Typical specimen configurations and the resulting temperature, composition, and melt density profiles during directional solidification of a binary alloy, (*b*) Pb-38 wt pct Sn (solidified downward); (*c*) Pb-38 wt pct Sn (solidified upward); (*d*) Pb-8 wt pct Au (solidified upward); and (*e*) Pb-8 wt pct Au (solidified downward).

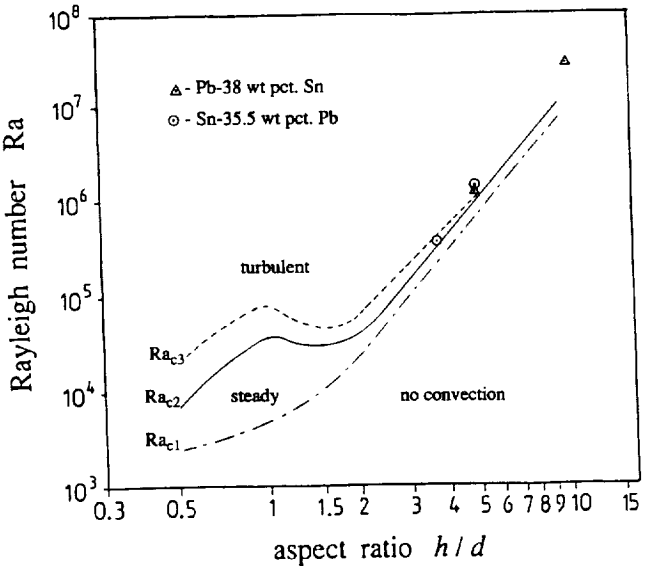

Fig. 12—Stability diagram of natural convection in low Prandtl number fluids in vertical insulated cylinders with the bottom hotter than the top.[17] Ra_{c1} is the critical Rayleigh number below which no convection occurs and above which steady-state convection develops. The solid line labeled Ra_{c2} indicates the transition from steady flow to time periodic flow, and Ra_{c3} is the critical Rayleigh number below which the convective mode is time periodic and above which the flow is unsteady turbulent, causing random temperature fluctuations in the melt.

respectively. Thus, as the magnetic field was increased, the phase shift between TC2 and 3 became longer, indicating that the flow velocities decreased with the application of the magnetic field. Further examination of the flow is being done numerically and will be presented in a later article.

C. *Elimination of Convection*

During directional solidification of alloys, the thermal and solutal gradients existing at the tips of the primary dendrite array, together with the alloy physical properties (liquid-solid surface energy and its anisotropy, solutal partition coefficient, and thermal and solutal diffusivities), determine the shape of the dendrite tips. The rest of the microstructural characteristics, such as the primary dendrite spacings, the microsegregation (composition of the melt at the tip and in the mushy zone), and the secondary dendrite spacings, may be correlated with tip shape. Therefore, the primary focus of the theories, both analytical and numerical,[28-35] has been to predict the shape of the primary dendrites as a function of the growth parameters and the alloy physical properties. These models consider only the diffusive thermal and solutal transports and do not include convection in their analyses due to the mathematical complexity of the situation. Our results, and examination of the literature on the constrained growth of binary metallic alloys, show that it is not feasible to avoid convection during terrestrial den-

dritic experiments. The terrestrial directional solidification experiments, whether upward growth or downward growth, whether with heavier solutes or lighter solutes, whether conducted with an applied magnetic field or without, are always accompanied by natural convection. It has not been possible to eliminate the convective transports and the associated problems in order to obtain the dendrite shapes which are determined by the diffusive transports only. Only low gravity directional solidification and quench experiments on well-characterized binary metallic alloys can yield the four critical parameters, the alloy growth speed, the shape of the primary dendrite tips (tip radius), the thermal gradient in the melt at the dendrite tips (G^l), and the solutal gradient at the dendrite tips (G_c^l), required for a meaningful evaluation of the dendrite growth models. Such experiments have not been carried out to date. Extensive research by Glicksman and his colleagues, including a recent low gravity experiment,[36] has demonstrated the significant influence of natural convection in determining the shape and growth behavior of free dendrites during their unconstrained growth. However, "free dendrite growth" experiments, such as Glicksman's, cannot be used to experimentally measure the four items, dendrite growth speed, tip radius, G^l, and G_c^l, independently, which is required for a quantitative evaluation of the dendrite growth theories in binary alloys. Only the two parameters, growth speed and tip shape, can be accurately measured by "free dendrite growth" experiments; the other two parameters are accessible only by calculations, which are themselves based upon the assumption that the theoretical model is valid. Directional solidification and quench experiments, on the other hand, can be used to independently measure all four parameters. It should also be pointed out that low gravity experiments,[37] for otherwise identical growth conditions, do not produce the dendrite "steeples" discussed previously, demonstrating that the convection in the vicinity of dendrite tips can be eliminated by low gravity.

V. CONCLUSIONS

1. Convection during downward growth, solid on top of the melt, can produce temperature fluctuations in the melt. With increasing instability, *i.e.*, a larger Rayleigh number, these fluctuations change from cyclic (time periodic with a constant frequency), to oscillatory (time periodic with several harmonics), and finally to random. Application of a transverse magnetic field partially suppresses these flows, as if the Rayleigh number had been decreased; the random flows tend to become oscillatory, and the oscillatory flows become cyclic. For the case of the lower temperature inversion, the 0.15 T transverse magnetic field changed the flow, changing the temperature fluctuations from sinusoidal to pulsed waves, characterized by a large spike in the temperature-time curve, and greatly decreasing the characteristic frequency of the flow.
2. In lieu of any applicable flow visualization and numerical modeling, the phase shifts present among the thermocouples are consistent with our conclusion that the fluctuations are caused by axial variations in flow velocity. This longitudinal flow is in the range of 4.8×10^{-3} m/s with no magnetic field and 1.1×10^{-3} m/s with 0.15 T applied.
3. The convective flow stability diagrams presented by others, relating thermal Rayleigh number, aspect ratio, and convection, are confirmed and in good agreement with our results.
4. Macrosegregation along the length of the directionally solidified specimens is produced only when the interdendritic liquid in the mushy zone convects and mixes with the bulk melt. Despite extensive convection in the bulk melt during downward growth of lead-rich (hypoeutectic) Pb-38 wt pct Sn, as evidenced by the thermal fluctuations, no longitudinal macrosegregation is observed because the interdendritic melt density profile is stabilizing. However, during upward growth of the same alloy, the interdendritic melt density profile destabilizes and extensive longitudinal macrosegregation results.

ACKNOWLEDGMENTS

Appreciation is expressed to the Microgravity Science and Applications Division for support of this research; to Ben Q. Li, Walter Duvall, and David A. Jacqmin for their helpful discussions; and to Thomas K. Glasgow, Chief, Processing Science and Technology Branch, for his assistance and use of experimental facilities at the NASA–Lewis Research Center.

REFERENCES

1. S.N. Tewari and R. Shah: *Metall. Trans. A*, 1992, vol. 23A, pp. 3383-92.
2. S.N. Tewari, R. Shah, and M.A. Chopra: *Metall. Trans. A*, 1993, vol. 24A, pp. 1661-69.
3. J. Verhoeven: *Metall. Trans.*, 1971, vol. 2, pp. 2673-80.
4. J.R. Sarazin and A. Hellawell: *Metall. Trans. A*, 1988, vol. 19A, pp. 1861-71.
5. W.J. Boettinger, F.S. Biancaniello, and S.R. Coriell: *Metall. Trans. A*, 1981, vol. 12A, pp. 321-27.
6. J.D. Verhoeven, J.T. Mason, and R. Trivedi: *Metall. Trans. A*, 1986, vol. 17A, pp. 991-1000.
7. S.N. Tewari and M.A. Chopra: *Microgravity Sci. Technol.*, 1990, vol. 3 (2), pp. 99-106.
8. R.M. Sharp and A. Hellawell: *J. Cryst. Growth*, 1970, vol. 10, pp. 29-32.
9. H. Jamgotchian, B. Billia, and L. Capella: *J. Crystal Growth*, 1987, vol. 82, pp. 342-50.
10. L. Wang, V. Laxmanan, and J.F. Wallace: *Metall. Trans. A*, 1988, vol. 19A, pp. 2687-94.
11. K.M. Kim, A.F. Witt, and H.C. Gatos: *J. Electrochem. Soc.: Solid-State Sci. Technol.*, 1972, vol. 119 (9), pp. 1218-26.
12. A.K. Sample and A. Hellawell: *Micro/Macro Scale Phenomena in Solidification*, C. Beckerman, L.A. Bertram, S.J. Pien, and R.E. Smelser, eds., ASME, Fairfield, NJ, 1992, ASME-HTD-vol. 218, pp. 73-84.
13. T.D. McCay, M.H. McCay, S.A. Lowry, and L.M. Smith: *J. Thermophysics Heat Transfer*, 1989, vol. 3 (3), pp. 345-50.
14. J.D. Verhoeven: *The Physics of Fluids*, 1969, vol. 12 (9), pp. 1733-40.
15. E.J. Harp and D.T.J. Hurle: *Phil. Mag.*, 1968, vol. 17, pp. 1033-38.
16. G. Muller, G. Neumann, and W. Weber: *J. Cryst. Growth*, 1984, vol. 70, pp. 78-93.
17. G. Muller: in *Crystals: Growth, Properties, and Applications*, Springer, Berlin, 1988, vol. 12.
18. J.R. Carruthers: *Preparation and Properties of Solid State Materials—Vol. 3*, W.R. Wilcox and R.A. Lefever, eds., Marcel Dekker, Inc., New York, NY, 1977, pp. 1-113.
19. H.C. de Groh III: *Metall. Mater. Trans. A*, 1994, vol. 25A, pp. 2507-16.
20. M.D. Dupouy, D. Camel, and J.J. Favier: *Acta Metall.*, 1989, vol. 37, pp. 1143-57.
21. S.N. Tewari, R. Shah, and H. Song: *Metall. Mater. Trans. A*, 1994, vol. 25A, 1535-44.

22. M.H. Burden, D.J. Hebditch, and J.D. Hunt: *J. Cryst. Growth*, 1973, vol. 20, pp. 121-24.
23. W.T. Mitchell and J.A. Quinn: *AICHE J.*, 1966, vol. 12, pp. 1116-24.
24. D.J. Knuteson, A.L. Fripp, G.A. Woodell, and W.J. Debnam, Jr.: *J. Cryst. Growth*, 1991, vol. 109, pp. 127-32.
25. *Liquid Metals*, S.Z. Beer, ed., Marcel Dekkar Inc., New York, NY, 1972, p. 186.
26. *Thermophysical Properties of Matter*, Y.S. Toloukian *et al.*, eds., TPRC Data Series Vols. 1, 4, and 11, Purdue Research Foundation, IFI/Plenum, New York, NY 1970.
27. W.R. Wilcox: in *Fractional Solidification*, M. Zief and W.R. Wilcox, eds., Dekkar, New York, NY, 1967, pp. 47-117.
28. M.H. Burden and J.D. Hunt: *J. Cryst. Growth*, 1974, vol. 22, pp. 109-16.
29. R. Trivedi: *Metall. Trans. A*, 1984, vol. 15A, pp. 977-82.
30. W. Kurz and D.J. Fisher: *Acta Metall.*, 1981, vol. 29, p. 11.
31. V. Laxmanan: *J. Cryst. Growth*, 1986, vol. 75, pp. 573-580.
32. J.S. Kirkaldy: *Scripta Metall.*, 1980, vol. 14, pp. 739-44.
33. P. Pelce and A. Pumir: *J. Cryst. Growth*, 1985, vol. 73, pp. 337-42.
34. L.H. Unger, M.J. Bennett, and R.A. Brown: *Phys. Rev. B*, 1985, vol. 31, pp. 5923-30.
35. J.D. Hunt and D.G. McCartney: *Acta Metall.*, 1987, vol. 35, pp. 89-99.
36. M.E. Glicksman: *Microgravity Materials Science Conf.*, Huntsville, AL, May 24–25, 1994.
37. M.D. Dupouy, D. Camel, and J.J. Favier: *Acta Metall.*, 1992, vol. 40 (7), pp. 1791-1801.